

# Hyper expression of MTBP may be an adverse signal for the survival of some malignant tumors

## A data-based analysis and clinical observation

Yantao Mao<sup>a</sup>, Mei Tian<sup>b</sup>, Bo Pan<sup>c</sup>, Qingshan Zhu<sup>d</sup>, Paiyun Li<sup>e</sup>, Hongmei Liu<sup>f</sup>, Weipeng Liu<sup>d</sup>, Ningtao Dai<sup>d</sup>, Lili Yu<sup>f</sup>, Yuan Tian, MD, PhD<sup>f,\*</sup>

### Abstract

To explore the relationship between mouse double minute 2 binding protein (MTBP) and the prognosis of cancer patients, a databank-based reanalysis was conducted and a clinical observation about lung adenocarcinoma was taken to verify the result of data analysis.

We reanalyzed all the downloaded data in order to make a conclusion about the relationship between MTBP and the prognosis of cancer patients. At last, we collected 112 lung cancer patients with MTBP information to verify the results of data analysis (GSE30219).

The overall Kaplan–Meier curve results of 6 eligible data groups were shown in Fig. 1. The Kaplan–Meier curve result of GSE16011 was shown in Fig. 1A (concordance index=59.48, Log-Rank Equal Curves [ $P=5.942e-05$ ],  $R^2=0.045/1$ , risk groups hazard ratio=1.69 [conf. int. 1.3–2.9],  $P=7.344e-05$ ), while the stratification results were displayed independently in Figs. 2 and 3. The similar results could be seen in other 5 data groups. The tissue sections of 112 patients with lung adenocarcinoma were collected and immunohistochemically stained. The hyper expression rate of MTBP in adenocarcinoma was 23.21% (26/112). The results showed that patients with hyper expression of MTBP had significantly worse prognosis than the control group, and the survival curves were clearly separated from each other (Fig. 4B,  $P=.000$ ).

Hyper expression of MTBP maybe an adverse event for the survival of some cancer patients, especially in glioblastoma, kidney cancer, and lung cancer patients, which has been verified in 112 lung cancer patients with MTBP status.

**Abbreviations:** CI = concordance index, GBM = Glioblastoma multiforme, GEO = Gene Expression Omnibus, HR = hazard ratio, MDM2 = mouse double minute 2, MTBP = mouse double minute 2 binding protein, OS = overall survival, PI = prognostic index, TCGA = The Cancer Genome Atlas.

**Keywords:** clinical observation, data-based analysis, malignant tumors, MTBP, prognosis

Editor: Jianxun Ding.

YM, MT, BP, and QZ have contributed equally to this work.

This study was funded by the Natural Science Foundation of Shandong Province (ZR2015HL078), which was in charged by Yuan Tian.

The authors have no conflicts of interest to disclose.

<sup>a</sup> Department of Oncology, Yantaishan Hospital of Shandong Province, Zhifu District, Yantai City, <sup>b</sup> Respiratory Department, Affiliated Hospital of Shandong University of Traditional Chinese Medicine, Jinan, Shandong, <sup>c</sup> Department of Lung Transplantation, First Affiliated Hospital, Zhejiang University School of Medicine, Hangzhou, <sup>d</sup> Department of Radiotherapy Oncology, Anyang Cancer Hospital of Henan Province, Anyang, Henan, <sup>e</sup> Division of Etiology, Peking University Cancer Hospital and Institute, Beijing, <sup>f</sup> Department of Radiation Oncology, Shandong Provincial Qianfoshan Hospital Affiliated to Shandong University, Jinan, Shandong, China.

\* Correspondence: Yuan Tian, Department of Radiation Oncology, Shandong Provincial Qianfoshan Hospital, No. 16766, Jingshi Road, Lixia District, Jinan City, Shandong Province 250014, China (e-mail: tytytianyuan@aliyun.com).

Copyright © 2018 the Author(s). Published by Wolters Kluwer Health, Inc. This is an open access article distributed under the terms of the Creative Commons Attribution-Non Commercial License 4.0 (CCBY-NC), where it is permissible to download, share, remix, transform, and buildup the work provided it is properly cited. The work cannot be used commercially without permission from the journal.

Medicine (2018) 97:35(e12021)

Received: 6 June 2018 / Accepted: 30 July 2018

<http://dx.doi.org/10.1097/MD.00000000000012021>

## 1. Introduction

Mouse double minute 2 (MDM2) binding protein (MTBP) is a protein, which interacts with oncoprotein murine double minute (MDM2), located in chr8:120445426-120523635, confirmed by in situ hybridization,<sup>[1]</sup> a major inhibitor of the tumor suppressor p53. It is reported to play a vital role in the regulation of the G(1) checkpoint of the cell cycle through its interaction with p53. p53-independent cell proliferation can be arrested by the expression level of MTBP, which is in turn blocked by simultaneous overexpression of MDM2.<sup>[2]</sup> Furthermore, MTBP may have some effects on tumor metastasis in mice and upregulate migratory potential of mouse embryonic fibroblasts regardless of the presence of p53.<sup>[3,4]</sup> With the development of science, more and more results showed that MTBP had p53-independent roles in tumorigenesis. Overexpression of MTBP is associated with poor prognosis of cancer patients.<sup>[5,6]</sup> Cordon-Cardo et al reported that soft tissue sarcoma and bladder cancer patients with tumors having both mutant p53 and overexpression of MTBP had a worse prognosis than those patients with tumors just harboring p53 mutations,<sup>[7]</sup> confirming that MDM2 played a p53-independent role in tumor development. Agarwal et al established an orthotopic tumor cell transplantation assay using osteosarcoma cells to indicate that MTBP suppresses cell migration and filopodia formation by inhibiting actinin-4 (ACTN4), which enhanced the understanding of MTBP in suppression of tumorigenesis and metastasis.<sup>[8]</sup>

In breast cancer specimens, overexpression of both MYC and MTBP was associated with a worse prognosis in 10-year survival of patients compared with MYC overexpression alone. MTBP was also frequently co-amplified with MYC in many human cancers. Mechanistic investigations implicated associations with TIP48/TIP49 as well as MYC in MTBP function in cellular transformation and the growth of human breast cancer cells. It means that MTBP functions with MYC to promote malignancy, identifying this protein as a novel general therapeutic target in human cancer. In a word, oncogenic protein MTBP interacts with MYC to promote tumorigenesis.<sup>[9]</sup> In hepatocellular carcinoma, MTBP was reported to inhibit migration and metastasis.<sup>[10]</sup> Thus, increasing evidence indicates the significance of MTBP in tumor progression. However, the relationship between MTBP and cancer patients was still poorly understood, especially in clinical practice. In order to conclude the role of MTBP among cancer patients, we downloaded the published data and made further analysis with the help of some online tools and data analysis software, then we collected histopathological sections of lung adenocarcinoma patients and performed immunohistochemical staining to further verify whether the results of the data analysis (GSE30219 and LUAD-TCGA) were correct.

## 2. Materials and methods

### 2.1. Data collection

We collected all the data mainly from International Cancer Genome Consortium, The Cancer Genome Atlas (TCGA), and Gene Expression Omnibus (GEO), selecting keywords related to MTBP, cancer, and gene expression technologies. For TCGA, all data were downloaded at the gene level (level 3). RNA-Seq counts data were  $\log^2$  transformed. The characteristics of all the available downloaded data were displayed in Table 1. A total of 112 lung adenocarcinoma tissue specimens and adjacent normal tissues were randomly collected from patients who received surgery for lung cancer at the Department of Cardiothoracic Surgery of An Yang Hospital of HeNan Province from January 2016 to February 2017 with the permission of Ethics Committee of our hospital. All the patients had not been treated with radiotherapy and chemotherapy before surgery. All tissues were histologically identified as adenocarcinoma, evaluated by 2 senior pathologists. Then, we took immunohistochemistry to make sure the expression status of MTBP protein.

### 2.2. Immunohistochemistry and evaluation of staining intensity

Formalin-fixed, paraffin-embedded tissues were cut into 4- $\mu\text{m}$ -thick slices, and were dewaxed in xylene, rehydrated, and graded ethanol solutions. Then, slices (4- $\mu\text{m}$  thick) were used for immunohistochemistry with a monoclonal anti-MTBP antibody (1:500 dilution, Abcam, Cambridge, UK). Antigens, heating the histopathological sections at 100°C for 35 minutes in citrate solution (10 mmol/L, pH 6.0), were reclaimed. Then sections were cooled and immersed in methanol in the presence of 0.3% hydrogen peroxide for 15 minutes to block the endogenous peroxidase activity, subsequently rinsed in phosphate buffer saline (PBS) for 5 minutes, according to the immunohistochemistry kit. PBS was taken as negative controls instead of the primary antibody. The sections were then incubated with horseradish

peroxidase-labeled goat against mouse/rabbit secondary antibody (Abcam). Diaminobenzene was adopted as the chromogen and hematoxylin as the nuclear counterstain. At last, slices were taken to be dehydrated, cleared, and mounted.

All of the staining was evaluated independently by 2 senior pathologists. In 10 randomly selected fields, the intensity of MTBP immunochemical staining and the percentage of stained cells were assessed. Intensity of expression was examined based on the MTBP immunopositivity of normal pneumocyte. Intensity of immunopositivity was classified as negative (absent; score 0), weak (decreased intensity, compared with normal pneumocytes; score 1), moderate (the same intensity as MTBP expression of normal pneumocytes; score 2), and strong (increased intensity, compared with MTBP expression of normal pneumocytes; score 3). Score 3 was defined as over-expression of MTBP.

### 2.3. Statistical analysis

We analyzed all the data with the help of online tools as bc-GeneExMiner, GOBO, PrognoScan, ITTACA, KMPlot, Recurrence Online, Stata, and SurvExpress. SPSS 19.0 software was used for clinical data statistical analysis. The relation between the MTBP in tumor specimens and other patient characteristics was examined with Pearson chi-squared test. Overall survival was calculated from the onset of initial diagnosis to the observation deadline or death. The log-rank test was taken to evaluate survival time for different groups. *P* values of clinical information shown are 2-sided, and *P* < .05 was considered statistically significant.

Prognostic index (PI) and Harrell's concordance index (CI) were taken to evaluate for all the downloaded data by Stata and R programming technology.<sup>[11–13]</sup> Harrell's CI (C index) was used to assess the discriminating ability of the different PIs. We adopt a means to identify the risk groups splitting the ordered PI (higher values corresponding to higher risk) and then let the same number of samples in each group mark the number of risk groups. If there are 2 risk groups, we will set the PI to the median. Another method of delineating risk groups is to adopt an optimization algorithm for the ordered PI. If there are 2 groups, the log-rank test will be performed along all values of the arranged PI. Then, the minimum *P* value is considered as the segmentation point for the algorithm, which was mentioned by Deguo Xu in his paper.<sup>[14]</sup>

This procedure is applicable to more than 2 groups, and a risk group is repeatedly optimized until no changes are found. All risk evaluation processes can be easily finished with online analysis tools, SPSS 19.0 software or Stata software.<sup>[15]</sup> In this survival analysis, the hazard ratio (HR) is the risk ratio of the terms stated by 2 levels of risk groups. Survival rate was plotted using Kaplan–Meier method and analyzed by using log-rank test method. The frequencies of categorical variables were compared using Pearson chi-squared or Fisher exact test, when appropriate. A value of *P* < .01 was considered to be statistical significant.

## 3. Results

Eleven thousand nine hundred seventy-three subjects with MTBP status information from 34 data groups, were shown and marked in Table 1, whereas 22 included data which just displayed without MTBP information. In order to reveal the relationship between MTBP and the survival of cancer patients, we analyzed all the data with survival information first. We tried our best to perform Kaplan–Meier survival curve for risk groups, CI, and *P*

**Table 1**  
**Characteristics and preliminary analysis results of all data.**

Tumor type	N	MTBP status	Database	Information of clinical data	No. of samples	Source	Overall survival (P value)
Malignant tumor of the brain	1	—	Lee Nelson Glioblastoma GSE13041 GPL96	Survival, age, gender	218	Lee	—
	2	+	Lee Nelson Glioblastoma GSE13041 GPL570	Survival, age, gender	27	Lee	.9533
	3	+	Phillips Aldape Astrocytoma GSE4271 GPL97	Survival, grade, age, gender	100	Phillips	.6126
	4	—	Phillips Aldape Astrocytoma GSE4271 GPL96	Survival, grade, age, gender	100	Phillips	—
	5	—	Freije Nelson Glioblastoma GSE4412 GPL96	Survival, grade, histology, age, gender	85	Freije	—
	6	+	Gravendeed French Glioblastoma GSE16011	Survival, histology, grade, therapy, gender, age	284	Gravendeed	7.344e−05
	7	+	Remke Medulloblastoma GSE28245	Survival, subtype, stage, gender, age	64	Remke	.272
	8	—	Glioblastoma multiforme TCGA	Survival	538	TCGA	—
	9	+	GBMLGG-TCGA Gliomas, June 2016	Survival	660	TCGA	4.4342e−12
	10	+	LGG-TCGA—low grade gliomas, June 2016	Survival	512	TCGA	3.053e−05
Malignant tumor of esophagus	1	—	Rao Giddings Esophagus GSE11595	Survival	34	Rao	—
	2	+	Peters C. Fitzgerald Esophagus GSE19417	Survival, nodes, histology, differentiation, tumor size, gender	76	Peters C	.1196
	3	+	ESCA-TCGA esophageal carcinoma, June 2016	Survival	184	TCGA	.986
Malignant tumor of ovarian	1	+	Tothill Bowtell Survival Ovarian GSE9891	Survival, relapse, stage, grade, age, subtype	285	Tothill	.6966
	2	+	Yoshihara Tanaka Ovarian GSE32062	Survival, recurrence, grade, stage, surgery	255	Yoshihara	.9924
	3	+	Crijns van der Ze Ovarian GSE13876	Survival, age	415	Crijns	.4203
	4	—	Nevins Bild Ovarian GSE3149	Survival, stage	153	Bild	—
	5	—	Ovarian metabase: 6 cohorts 22K genes	Survival	784	SurvExpress	—
	6	—	Ovarian serous cystadenocarcinoma TCGA	Survival, relapse, stage	578	TCGA	—
	7	+	OV-TCGA—ovarian serous cystadenocarcinoma, June 2016	Survival	247	TCGA	.9616
Malignant tumor of stomach	1	+	Stomach adenocarcinoma TCGA	Survival, grade, stage	57	TCGA	.3421
	2	+	STAD-TCGA—stomach adenocarcinoma, June 2016	Survival	352	TCGA	.9497
	3	+	STES-TCGA—stomach and esophagus adenocarcinoma	Survival	440	TCGA	.4788
Malignant tumor of uterine	1	+	Uterine Corpus Endometrioid Carcinoma TCGA	Survival, figo stage, grade	332	TCGA	.2999
	2	+	UCEC-TCGA—uterine corpus endometrial carcinoma, June 2016	Survival	247	TCGA	.02526
	3	+	UCS-TCGA—uterine carcinosarcoma, June 2016	Survival	56	TCGA	.528
Malignant tumor of breast	1	+	Breast Invasive Carcinoma TCGA	Survival, stage, ER, PR	502	TCGA	.1628
	2	—	Wang Foekens Breast GSE2034	Recurrence, ER, treatment, node	286	Wang	—
	3	—	Sotiriou Van de Vijver Breast GSE2990	Recurrence, ER, treatment, node	189	Sotiriou	—
	4	—	Loi Sotiriou Breast GSE6532	Recurrence, ER, treatment, grade, node	225	Loi	—
	5	—	Breast Cancer Metabase: 10 cohorts 22K genes	Recurrence, ER status, LN status, meta-analysis	1901	SurvExpress	—
	6	—	Miller Bergh Breast GSE3494-GPL96	Survival, ER, PR, grade, size, node, age	502	Miller	—
	7	—	Staaf Borg Breast GSE25307	Survival, ER, PR, subtype, grade, PAM50, BRCA	577	Jönsson	—
	8	+	Prat-Perou-Breast-GSE18229	Relapse free survival, overall free survival, ER, nodes, PAM50	254	Prat	.2146
	9	+	Wang Leong Breast GSE45725	Recurrence, age, tumor, margin, location, size	340	Wang	.3187
Malignant tumor of kidney	1	—	Zhao Renal Kidney GSE3538	Survival, stage, grade, age, gender	177	Zhao	—
	2	+	Kidney renal clear cell carcinoma TCGA	Survival, grade, stage	468	TCGA	.07053

(continued)

**Table 1**  
(continued).

Tumor type	N	MTBP status	Database	Information of clinical data	No. of samples	Source	Overall survival (P value)
	3	+	<a href="#">KIPAN-TCGA Kidney PAN cancer TCGA, June 2016</a>	<a href="#">Survival</a>	<a href="#">792</a>	<a href="#">TCGA</a>	<a href="#">.1062e-05</a>
	4	+	KIRC-TCGA, kidney renal clear cell carcinoma	Survival	415	TCGA	.02724
	5	+	KIRP-TCGA, kidney renal papillary cell carcinoma, June 2016	Survival	278	TCGA	.08281
Malignant tumor of pancreatic	1	+	Stratford Yeh Pancreatic GSE21501	Survival, stage	132	Stratford	.9641
	2	+	PACA-AU-ICGC—pancreatic cancer-ductal adenocarcinoma, June 2016	Survival	189	ICGC	.08103
Malignant tumor of bladder	1	+	Leem Kim Bladder GSE13507	Survival, overall survival, gender, age, stage, progression, therapy	246	Kim	.6265
	2	+	BLCA-TCGA—bladder urothelial carcinoma, July 2016	Survival	390	TCGA	.1428
Malignant tumor of liver	1	+	TCGA-Liver-Cancer	Overall survival, recurrence free survival	422	TCGA-Research	.2936
	2	+	LIHC-TCGA—liver hepatocellular carcinoma, June 2016	Survival	361	TCGA	.7561
Malignant tumor of colon	1	+	Jorissen Sieber Colon Cancer Survival GSE14333	Survival, stage, age, gender	290	Jorissen	.8378
	2	—	Colon-Metabase-Uniformized	Disease free, specific and overall survival, age, gender, ethnicity	947	GSE12945-Staub	—
	3	+	COADREAD-TCGA Colon and Rectum adenocarcinoma, June 2016	Survival	467	TCGA	.6397
Malignant tumor of head and neck	1	+	Head and neck squamous cell carcinoma TCGA	Survival, grade, stage	283	TCGA	.1259
	2	+	HNSC-TCGA Head and Neck squamous cell carcinoma, June 2016	Survival	502	TCGA	.1054
Malignant tumor of lung	1	—	Directors Challenge Consortium NCI Lung	Survival, grade, stage, smoking, age, gender	462	Kerby	—
	2	+	Okayama Kohno Lung GSE31210	Survival, smoke, age, gender	226	Kohno	.2238
	3	+	<a href="#">LUAD-TCGA—lung adenocarcinoma, June 2016</a>	<a href="#">Survival</a>	<a href="#">475</a>	<a href="#">TCGA</a>	<a href="#">.01011</a>
	4	+	<a href="#">Rousseaux GSE30219</a>	<a href="#">Survival, histology, gender, stage</a>	<a href="#">264</a>	<a href="#">Rousseaux</a>	<a href="#">1.745e-05</a>

Characteristics of all data.

MTBP = mouse double minute 2 binding protein

$P \leq .05$  was considered to be statistically significant.

value of the log-rank testing equality of survival curves in every database with MTBP information, as recommended by Bovelstad and Borgan.<sup>[16]</sup> Among all the results, green color represents low-risk groups and red color means high-risk groups. Of 34 data groups, 6 showed the statistical significant  $P$  value, which were marked in Table 1. Kaplan–Meier survival curves of 6 risk groups can be seen in Fig. 1. We conclude from the preliminary results that hyper expression of MTBP may be associated with the worse prognosis of glioblastoma, kidney cancer, and lung cancer patients.

The stratification analysis of GSE16011 was made according to survival, histology, grade, therapy, gender, and age of the tumor data. The overall Kaplan–Meier curve result was shown in Fig. 1A (CI=59.48, Log-Rank Equal Curves [ $P=5.942e-05$ ],  $R^2=0.045/1$ , risk groups HR=1.69 [conf. int. 1.3–2.9],  $P=7.344e-05$ ), while the stratification results were displayed independently in Figs. 2 and 3. Figure 2A showed clinical information available related to risk group, PI, and outcome data, while a box plot across risk groups, including the  $P$  value testing for difference using  $t$  test was shown in Fig. 2C. The process of risk group optimization was displayed in Fig. 2B. The Log-Rank Equal Curves were obviously separated from each other in Fig. 2E (CI=61.27, Log-Rank Equal Curves [ $P=.0005411$ ],  $R^2=0.059/0.998$ , risk groups HR=2.21 [conf. int. 1.39–3.49],

$P=.0007378$ ) compared with Fig. 2D and F, when all the patients were grouped by gender. Then, the data of GSE16011 were taken into stratification by tumor grade and surgery. The results were gathered in Fig. 3. Log-Rank Equal Curves were shown in separated trend just in Fig. 3C, stratified by grade, while all the results were of no statistical significance. In the subgroup of partial resection, shown in Fig. 3F, Log-Rank Equal Curves were separated obvious from each other (CI=59.62, Log-Rank Equal Curves [ $P=5.408e-05$ ],  $R^2=0.052/0.999$ , risk groups HR=2.07 [conf. int. 1.44–2.97],  $P=7.671e-05$ ), when the subgroups were divided by surgery type.

Similar stratification of GSE30219, relating to lung cancer, was put into practice by stage of adenocarcinoma. The overall Log-Rank Equal Curve was exhibited in Fig. 1F (CI=62.47, Log-Rank Equal Curves [ $P=1.189e-05$ ],  $R^2=0.063/0.998$ , risk groups HR=1.99 [conf. int. 1.45–2.73],  $P=1.745e-05$ ), while the details of the stratification results were provided in Fig. 4. The Log-Rank Equal Curves were obviously separated from each other in Fig. 4B (CI=62.05, Log-Rank Equal Curves [ $P=.000419$ ,  $R^2=0.051/0.993$ , risk groups HR=2.02 [conf. int. 1.36–3.00],  $P=.000544$ ) compared with others.

All the above results are just concluded from data analysis. In order to verify the authenticity and correctness of the above

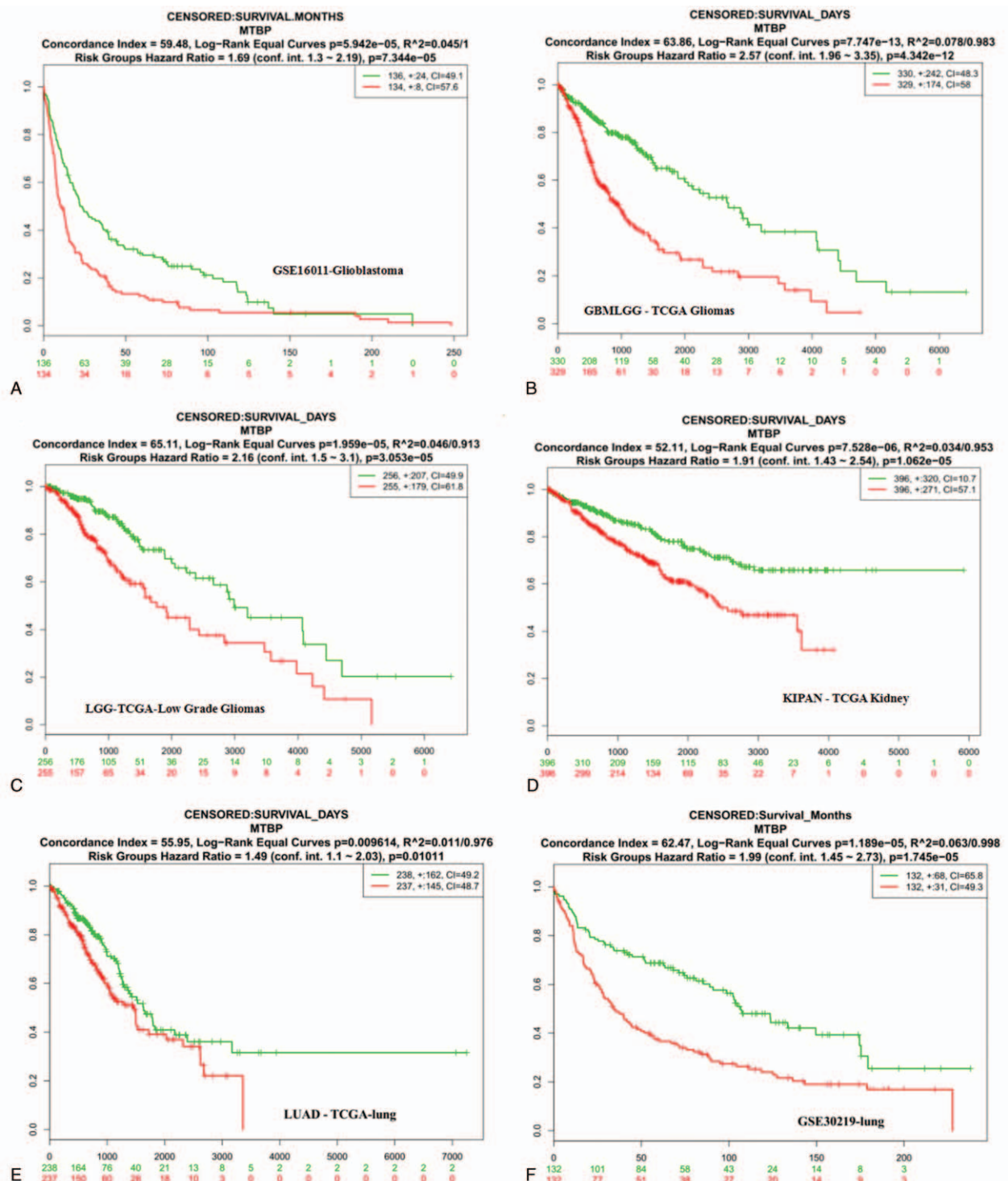


**Figure 1.** Kaplan-Meier survival curve for 6 risk groups, concordance index (CI), and *P* value of the log-rank testing equality of survival curves in every database. Red and green curves denote high- and low-risk groups, respectively. The ordinal (Y-axis) indicates the percentage of survival, the abscissa (X-axis) represents survival days, and the number of survivors at the corresponding time. Censoring samples are shown as “+” marks. The number of individuals, the number of censored, and the CI of each risk group are shown in the top-right insets. (A) Kaplan-Meier survival curve for Glioblastoma GSE16011. (B) Kaplan-Meier survival curve for GBMLGG-TCGA Gliomas. (C) Kaplan-Meier survival curve for LGG-TCGA—low-grade gliomas. (D) Kaplan-Meier survival curve for KIPAN-TCGA—kidney cancer. (E) Kaplan-Meier survival curve for LUAD-TCGA—lung adenocarcinoma. (F) Kaplan-Meier survival curve for Rousseaux GSE30219—lung cancer.

results, especially in GSE30219, we retrospectively collected 112 cases of lung adenocarcinoma patients for further clinical validation. Patient characteristics were gathered in Table 2. Expression status of MTBP gene was determined by immunohistochemistry. The results of immunohistochemical staining for

pathological tissue sections of lung cancer were shown in Fig. 5, including normal tissue (Fig. 5A and B) and adenocarcinoma tissue (Fig. 5C–E). The overexpression status of MTBP gene was displayed in Fig. 5E, marked as (+++). Overall, 49 patients were female and 63 were male. Twenty-six patients were shown to be

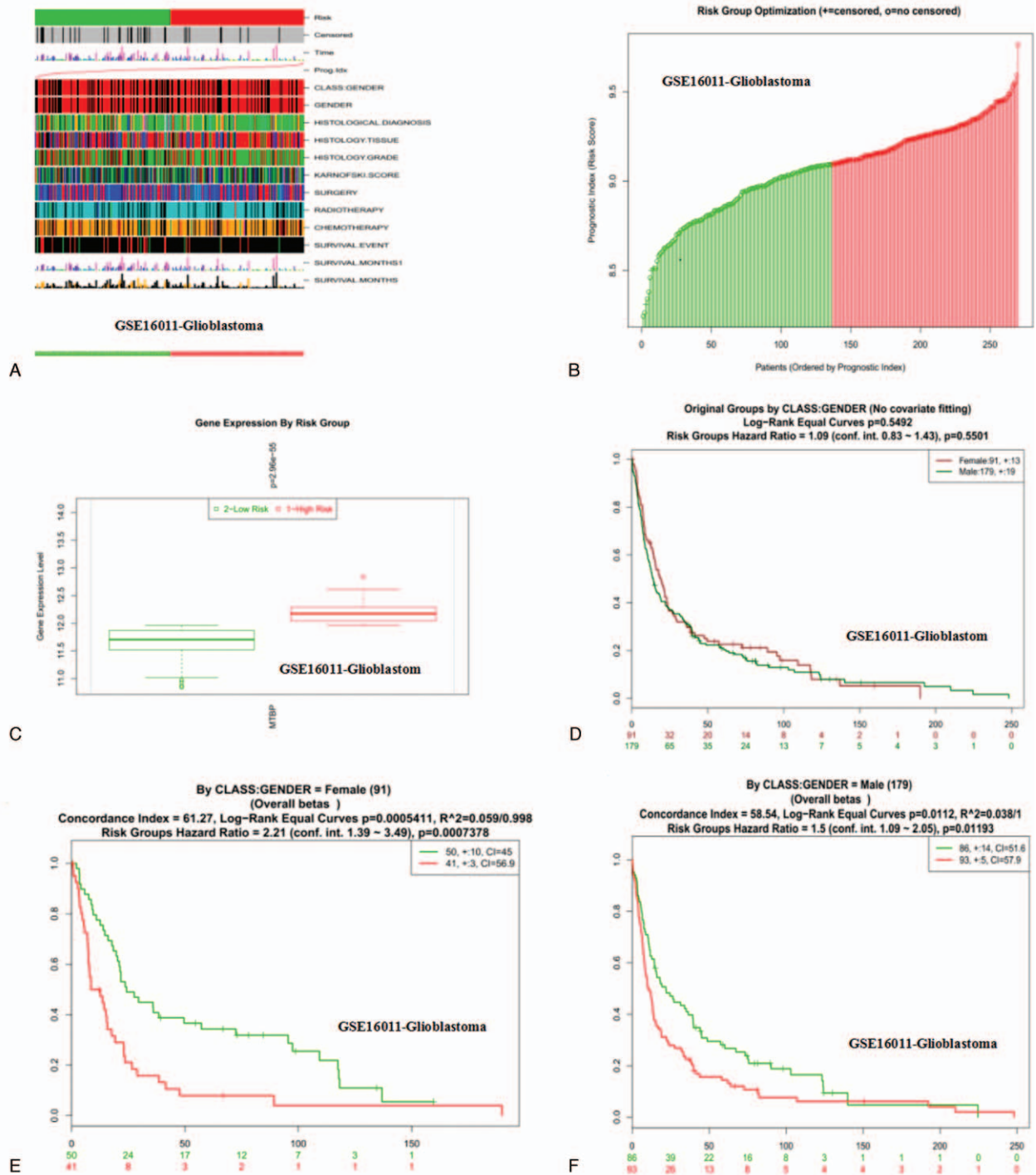


**Figure 2.** Kaplan–Meier survival curves and performance of stratification analysis in Glioblastoma GSE16011 according to tumor grade and surgical approach. Red and green curves denote high- and low-risk groups, respectively. The ordinal (Y-axis) indicates the percentage of survival, the abscissa (X-axis) represents survival days, and the number of survivors at the corresponding time. Censoring samples are shown as “+” marks. The number of individuals, the number of censored, and the CI of each risk group are shown in the top-right insets. (A) Clinical information available related to risk group, prognostic index, and outcome data. (B) The censored process of risk group optimization by prognostic index. (C) Box plot across risk groups, including the *P* value testing for difference using *t* test (or *f*-test for more than 2 groups). The ordinate (Y-axis) indicates the expression percentage of the gene, the abscissa (X-axis) represents different risk groups. (D) Performance of stratification analysis for original groups by class: gender (no covariate fitting). (E) Performance of stratification analysis by gender=female. (F) Performance of stratification analysis by gender=male. CI = concordance index.

associated with hyper expression of MTBP protein. The hyper expression rate of MTBP was obvious higher in the subgroup of ECOG, stage and pleural effusion, which the *P* value of them were of statistical significance. Then, the survival analysis of 112

lung adenocarcinoma patients was put into practice. Clinical tumor stage, overexpression of MTBP, and malignant pleural effusion, shown in Fig. 6A–C, are factors that have the most significant influence on the prognosis of patients. The Kaplan–

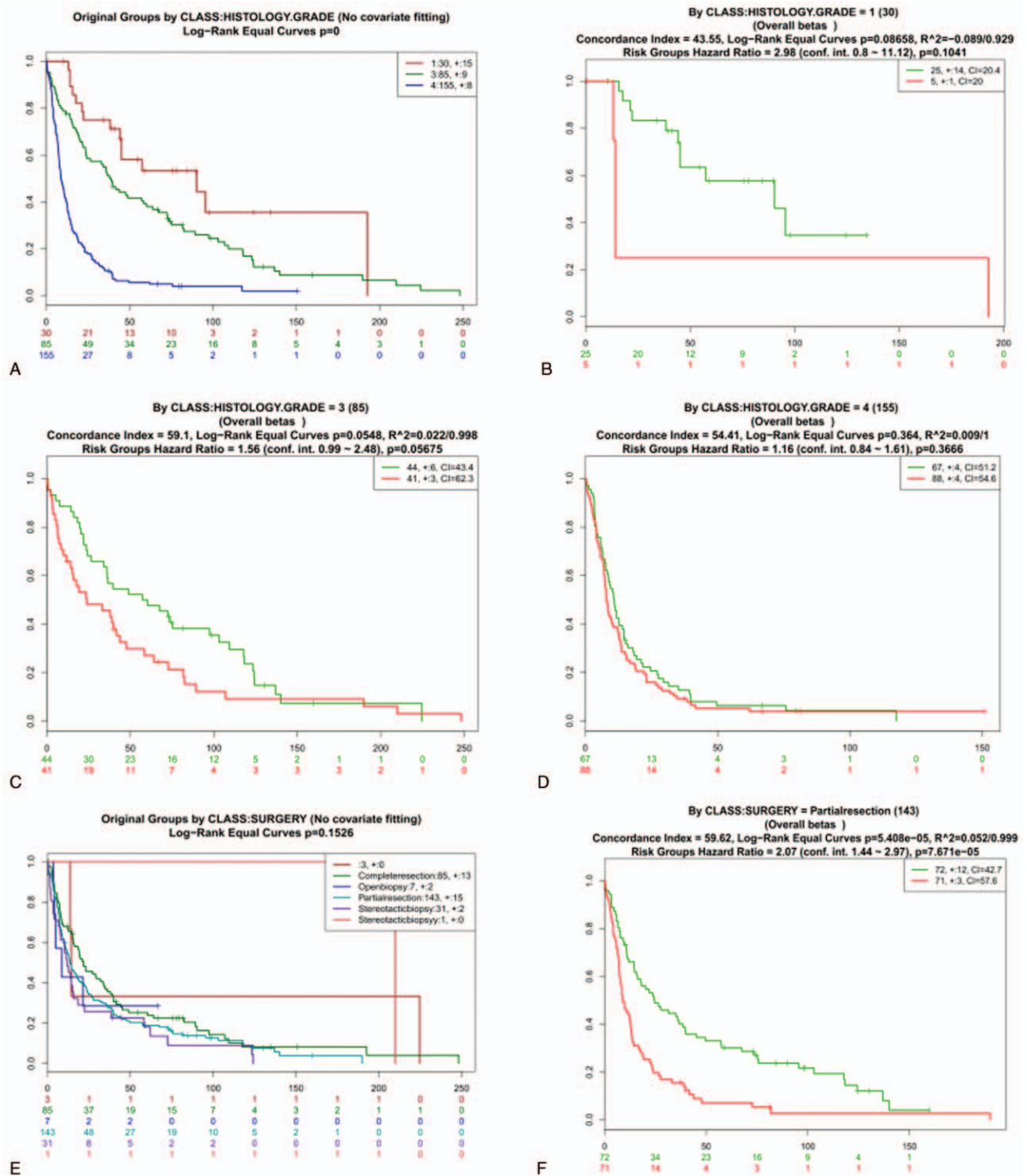


**Figure 3.** Performance of stratification analysis in Glioblastoma GSE16011 according to tumor grade and surgical approach. Red and green curves denote high- and low-risk groups, respectively. The ordinal (Y-axis) indicates the percentage of survival, the abscissa (X-axis) represents survival days, and the number of survivors at the corresponding time. Censoring samples are shown as “+” marks. The number of individuals, the number of censored, and the CI of each risk group are shown in the top-right insets. (A) Performance of stratification analysis for original groups by class: histology-grade (no covariate fitting). (B) Kaplan–Meier curves and performance of stratification analysis by grade 1. (C) Kaplan–Meier curves and performance of stratification analysis by grade 3. (D) Kaplan–Meier curves and performance of stratification analysis by grade 4. (E) Kaplan–Meier curves and performance of stratification analysis for original groups by class: surgery (no covariate fitting). (F) Kaplan–Meier curves and performance of stratification analysis by partial resection. (G) Kaplan–Meier curves and performance of stratification analysis by stereotactic biopsy. (H) Kaplan–Meier curves and performance of stratification analysis by complete resection. CI = concordance index.

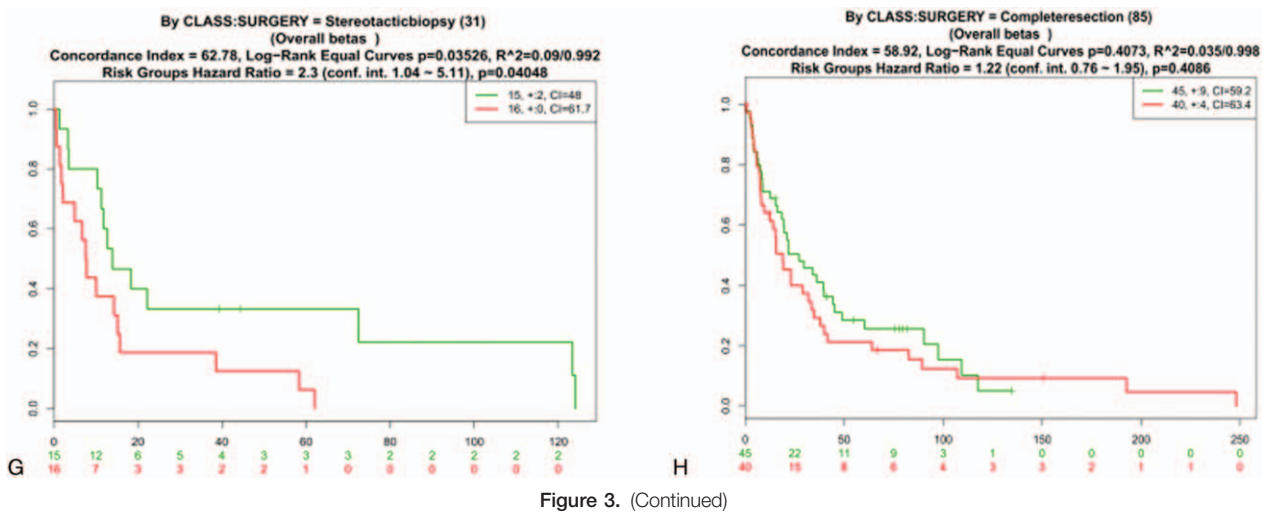
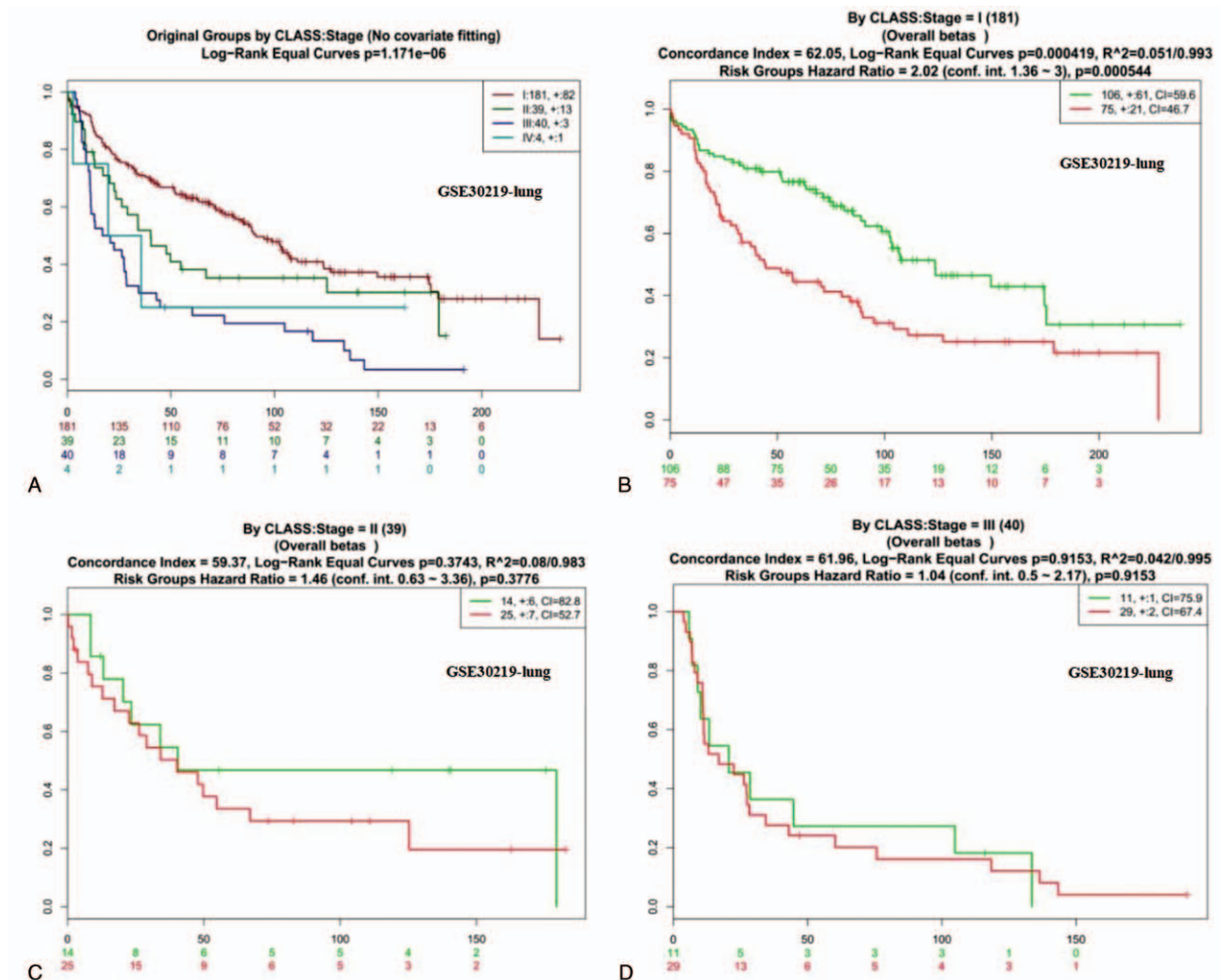


Figure 3. (Continued)



**Figure 4.** Performance of stratification analysis for Rousseau GSE30219. Red and green curves denote high- and low-risk groups, respectively. The ordinal (Y-axis) indicates the percentage of survival, the abscissa (X-axis) represents survival days, and the number of survivors at the corresponding time. Censoring samples are shown as “+” marks. The number of individuals, the number of censored, and the CI of each risk group are shown in the top-right insets. (A) Kaplan–Meier survival curves and performance of stratification analysis for original groups by Class: stage (no covariate fitting). (B) Kaplan–Meier curves and performance of stratification analysis by Class: stage=I. (C) Kaplan–Meier curves and performance of stratification analysis for original groups by Class: stage=II. (D) Kaplan–Meier curves and performance of stratification analysis by Class: stage=III. CI = concordance index.

**Table 2**  
**Clinical characteristics of 112 patients with lung cancer.**

Tumor type	N	MTBP status (%)	Pearson chi-squared (P value)
Age			
≤60	60	14 (23.3)	.974
>60	52	12 (23.1)	
Sex			
Male	63	18 (28.6)	.128
Female	49	8 (16.3)	
Smoking status			
Yes	31	9 (29.0)	.367
Never	81	17 (21.0)	
ECOG			
0	51	6 (11.8)	.009
1/2	61	20 (32.8)	
Stage			
I-II	27	2 (7.4)	.008
III	36	6 (16.7)	
IV	49	18 (36.7)	
Treatment (first line)			
Docetaxel + platinum	45	9 (20.0)	.139
Pemetrexed + platinum	35	5 (14.3)	
Tyrosine kinase inhibitor	24	9 (37.5)	
No	8	3 (37.5)	
Pleural effusion			
Yes	18	8 (44.4)	.020
No	94	18 (19.1)	

ECOG=eastern cooperative oncology group, MTBP status (%)=proportion of patients with hyper expression of MTBP, MTBP=mouse double minute 2 binding protein. P< .05 was considered to be statistically significant.

Meier survival curves were obviously separated from each other, which the results of Fig. 6B are similar to the results of data group GSE30219. Patients receiving treatment had a better prognosis than patients who had not received any treatment (Fig. 6D), while the differences among 3 treatment approaches, compared in pairs, were of no obvious significance (P=.305/.457/.957).

### 4. Discussion

As is known to all, Glioblastoma multiforme (GBM) is an aggressive, invasive brain tumor with poor prognosis.<sup>[17]</sup> Although, surgical resection and chemoradiotherapy are taken to deal with GBM, 5-year survival rate is no more than 5% after initial diagnosis.<sup>[18]</sup> Conventional chemotherapy shows lower survival benefits in GBM patients because of poor blood-brain barrier penetration, tumor heterogeneity, intrinsic resistance, and nonspecific toxicity.<sup>[19]</sup> A lot of clinical trials were carried out in the past years, but the survival of patients had been improved little.<sup>[20]</sup> A lot of factors are thought to be associated with the development of gliomas, but the pathogenesis of gliomas is still to be further studied.<sup>[21,22]</sup> Therefore, plenty of further researches are urgently required to find out novel therapeutic targets and develop more effective combination strategies for GBM treatment.

MTBP is a protein, which interacts with oncoprotein murine double minute (MDM2), a major inhibitor of the tumor suppressor p53.<sup>[11]</sup> It was reported to be associated with cancer in some mechanism research,<sup>[8-10,23]</sup> scarcely involved in clinical trials. With the development of whole genome sequencing, more and more scientific problems related to pathogenic genes can be elucidated.<sup>[24-26]</sup> However, the expenditure of sequencing is too high to be widely used for every research team. So, we change the perspective of our study instead of sequencing. Plenty of data about MTBP related to cancers can be downloaded online, such as TCGA, GEO, and so on. We reanalyzed the downloaded data (17,517 samples) to make sure the relationship between the level of MTBP expression and the survival of cancer patients. The overall Log-Rank Equal Curves were obvious separated from each other in 6 data groups, especially in glioblastoma patients (involved 1396 samples), which P values of them were all of statistical significance. The detail of the results can be seen in Fig. 1. Therefore, we can conclude from the preliminary result that MTBP gene may be an adverse signal for the survival of glioblastoma, kidney cancer, and lung adenocarcinoma cancer patients.

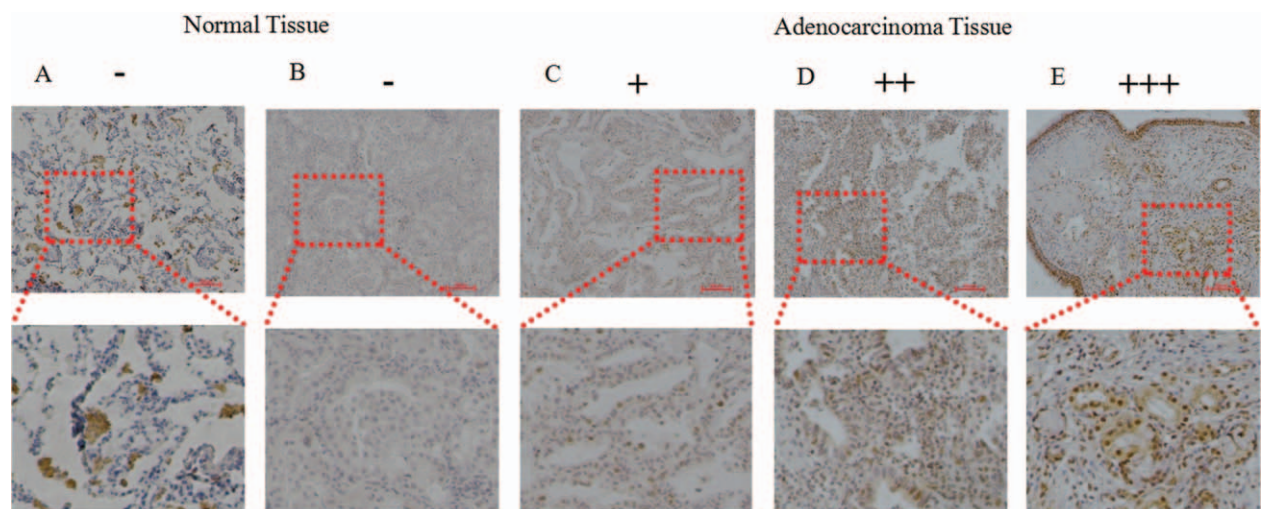


**Figure 5.** Immunohistochemical staining results of normal and adenocarcinoma tissues. (A, B) Immunohistochemistry results of normal tissue. (C) Immunohistochemical staining results of adenocarcinoma tissues, marked as (+). (D) Immunohistochemical staining results of adenocarcinoma tissues, marked as (++) . (E) Immunohistochemical staining results of adenocarcinoma tissues, marked as (+++), which was defined for hyper expression or over expression of mouse double minute 2 binding protein.

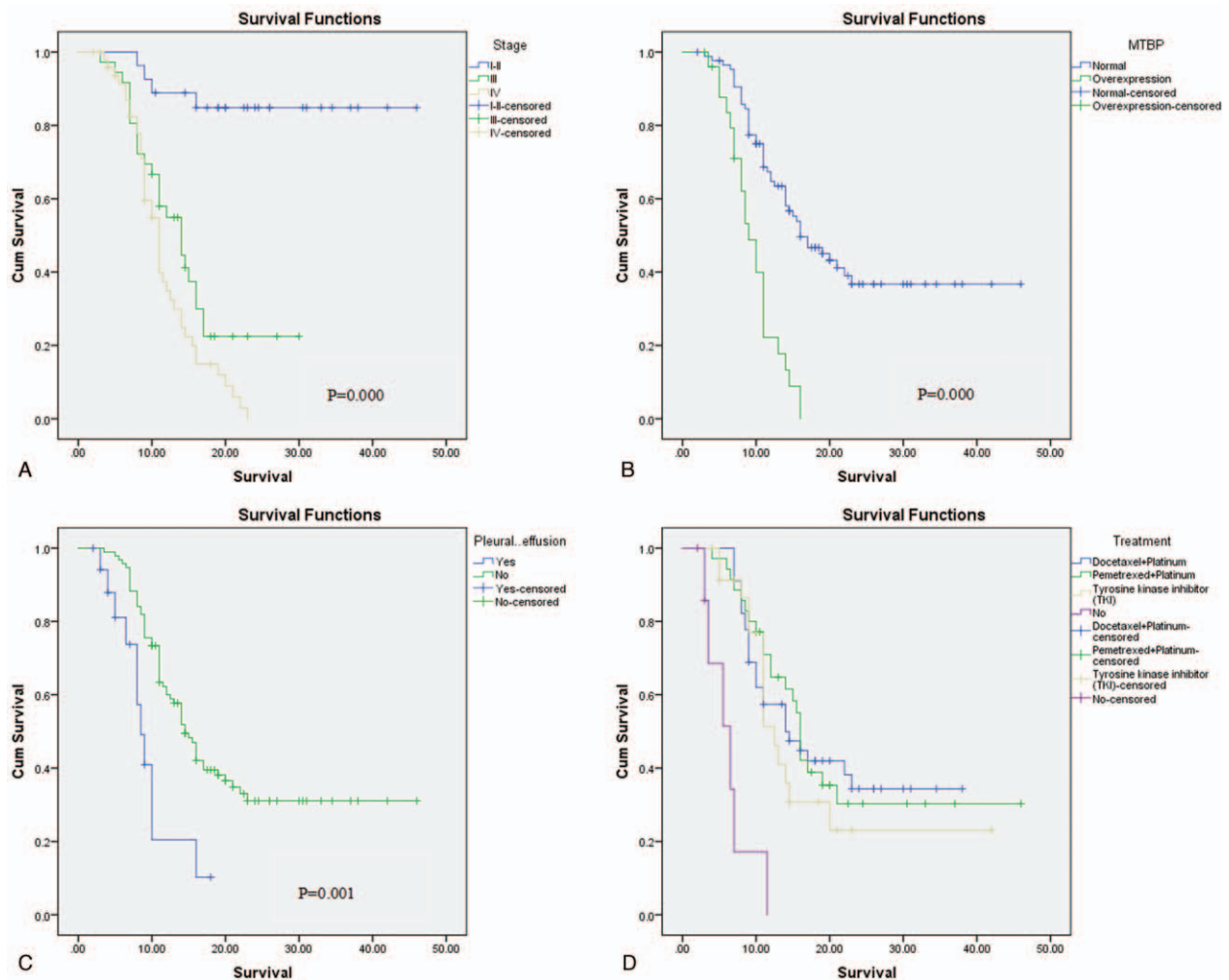


**Figure 6.** Kaplan–Meier curves and performance of stratification analysis for 112 lung cancer patients. (A) Kaplan–Meier curves for original groups by stage. (B) Kaplan–Meier curves of analysis by status of mouse double minute 2 binding protein. (C) Kaplan–Meier curves of analysis by status of pleural effusion. (D) Kaplan–Meier curves and performance of stratification analysis by treatment methods.

GBM could be divided into mesenchymal, classical, neural, and proneural subtypes according to a gene expression-based molecular classification system, created by TCGA.<sup>[27]</sup> Three signaling pathways are frequently reported in GBM: receptor tyrosine kinase (RTK)/Ras/phosphoinositide 3-kinase (PI3K), p53, and retinoblastoma (Rb) signaling. These have led to a better understanding of the molecular mechanism of GBM and have revealed numerous important changes in genes and pathways,<sup>[28,29]</sup> scarcely involved MTBP. MTBP is a major inhibitor of the tumor suppressor p53.<sup>[11]</sup> It may show its effects on GBM through p53 signal pathway. In order to get more information about MTBP, we put the data of GSE16011 into stratification. The results were gathered in Figs. 2 and 3. Furthermore, some of the results, listed in Figs. 2E and 3F, supported our hypothesis that overexpression of MTBP is an adverse signal for the survival of glioblastoma patients.

Every year, there are almost 270,000 patients suffering from kidney cancer leading to 11,500 deaths.<sup>[30]</sup> A lot of genes linked with kidney cancer, such as VHL, MET, FLCN, TSC1, TSC2, NOD2, and TFE3,<sup>[14]</sup> were identified by genome researches and have significantly changed the ways in which patients with kidney cancer are treated. The VHL pathway had been admitted for the therapy of patients with advanced kidney cancer. More new

genome researches, such as whole genome sequencing, gene expression patterns, and so on, will still be needed to carried out to get a complete understanding of the genetic basic mechanism of kidney cancer and the kidney cancer gene pathways and, most importantly, to provide the foundation for the development of effective forms of therapy for patients with the disease.<sup>[31]</sup> The Log-Rank Equal Curve of KIPAN, displayed in Fig. 1D, revealed that expression of MTBP is bad for the survival of kidney patients, which may provide useful guidance for kidney cancer treatments in the future. MTBP may be a new therapy target for kidney cancer patients, though plenty of researches are still needed to elucidate the mechanism between MTBP and the prognosis of kidney cancers.

There are plenty of genes or RNA involved in the tumorigenesis of lung cancer, including PD-1, K-RAS, EGFR, VEGF, BRAF, ERK-2, which promotes the development of lung cancer treatments.<sup>[32–37]</sup> However, it is the first time for the relationship between MTBP expression and the survival of lung cancer patients to be revealed by reanalysis of online sequencing data, shown in Fig. 1F (CI=62.47, Log-Rank Equal Curves [ $P=1.189e-05$ ],  $R^2=0.063/0.998$ , risk groups HR = 1.99 [conf. int. 1.45–2.73],  $P=1.745e-05$ ). It confirmed the relationship between MTBP expression and the survival of lung cancer

patients, and displayed that overexpression of MTBP is an adverse event for the prognosis of patients. The stratification of GSE30219 was carried out according to stage and histology of the tumor, which revealed that the Log-Rank Equal Curves were separated from each other in subgroup of adenocarcinoma and stage I, listed in Fig. 4.

The above results are picked up only from simple data analysis, and the authenticity and credibility are still to be verified. Therefore, we selected 112 cases of lung adenocarcinoma patients clinical pathological sections for immunohistochemical staining, to further verify the reality of the above conclusions. Patient characteristics were summarized in Table 2. Clinical tumor stage, overexpression of MTBP, and malignant pleural effusion, shown in Fig. 6A–C, are factors that have significant influence on the prognosis of patients, which the results of Fig. 5B are consistent with the results of data group GSE30219. It was further confirmed that MTBP gene hyper expression is unfavorable to the prognosis of lung adenocarcinoma cancer patients. Every year, the College of American Pathologists, the International Association for the Study of Lung Cancer, and the Association for Molecular Pathology will update their recommendations for molecular testing for the selection of patients with lung cancer for treatment with targeted tyrosine kinase inhibitors.<sup>[38,39]</sup> EGFR status is always listed as the first recommended test. It means that effective biological predictors, such as EGFR, ROS-1, ALK, and so on, are extremely important for evaluating the prognosis of cancer patients.<sup>[40–42]</sup> Through the above data analysis results and some clinical validation results, we can infer that MTBP, similar to EGFR, may become an indicator to evaluate the prognosis of cancer in the future, especially in lung adenocarcinoma cancer patients. More basic research on MTBP gene and clinical validation trials need to be invested in order to further clarify the role of MTBP in the development, progression, and prognosis of cancer.

## 5. Conclusions

We can conclude that hyper expression of MTBP is an adverse event for the survival of glioblastoma, kidney cancer, and lung cancer patients, which has been clinically verified in lung cancer.

### 5.1. Ethical approval

We declared that all procedures involved in this study about human participants were in accordance with the ethical standards of the institutional and/or national research committee and with the 1964 Helsinki declaration and its later amendments or comparable ethical standards. For this type of study formal consent is not required.

## Author contributions

Yuan Tian was responsible for the final decision to submit for publication or others. Yantao Mao and Mei Tian had the full data of the paper. Bo Pan helped to gather data and write the report. Lili Yu and Hongmei Liu helped with study design, data collection.

**Data curation:** Mei Tian, Qingshan Zhu, Hongmei Liu, Weipeng Liu, Ningtao Dai, Lili Yu.

**Formal analysis:** Yantao Mao, Bo Pan, Qingshan Zhu, Hongmei Liu, Weipeng Liu, Ningtao Dai, Yuan Tian.

**Funding acquisition:** Yuan Tian.

**Project administration:** Yuan Tian.

**Resources:** Paiyun Li, Lili Yu.

**Software:** Paiyun Li, Weipeng Liu.

**Writing – original draft:** Yuan Tian.

**Writing – review & editing:** Mei Tian, Ningtao Dai.

## References

- [1] Boyd MT, Zimonjic DB, Popescu NC, et al. Assignment of the MDM2 binding protein gene (MTBP) to human chromosome band 8q24 by in situ hybridization. *Cytogenet Cell Genet* 2002;90:64–5.
- [2] Boyd MT, Vlatkovic N, Haines DS. A novel cellular protein (MTBP) binds to MDM2 and induces a G1 arrest that is suppressed by MDM2. *J Biol Chem* 2000;275:31883–90.
- [3] Iwakuma T, Tochigi Y, Van Pelt CS, et al. MTBP haploinsufficiency in mice increases tumor metastasis. *Oncogene* 2008;27:1813–20.
- [4] Iwakuma T, Agarwal N. MDM2 binding protein, a novel metastasis suppressor. *Cancer Metastasis Rev* 2012;31:633–40.
- [5] Lu ML, Wikman F, Orntoft TF, et al. Impact of alterations affecting the p53 pathway in bladder cancer on clinical outcome, assessed by conventional and array-based methods. *Clin Cancer Res* 2002;8:171–9.
- [6] Bouska A, Eischen CM. Murine double minute 2: p53-independent roads lead to genome instability or death. *Trends Biochem Sci* 2009;34:279–86.
- [7] Cordon-Cardo C, Latres E, Drobnjak M, et al. Molecular abnormalities of MDM2 and p53 genes in adult soft tissue sarcomas. *Cancer Res* 1994;54:794–9.
- [8] Agarwal N, Adhikari AS, Iyer SV, et al. MTBP suppresses cell migration and filopodia formation by inhibiting ACTN4. *Oncogene* 2013;32:462–70.
- [9] Grieb BC, Gramling MW, Arrate MP, et al. Oncogenic protein MTBP interacts with MYC to promote tumorigenesis. *Cancer Res* 2014;74:3591–602.
- [10] Bi Q, Ranjan A, Fan R, et al. MTBP inhibits migration and metastasis of hepatocellular carcinoma. *Clin Exp Metastasis* 2015;32:301–11.
- [11] Collett D. *Modelling Survival Data in Medical Research*. 1993; Chapman and Hall/CRC, 368 pp.
- [12] Harrell FE Jr. *Regression Modeling Strategies, With Applications to Linear Models, Logistic Regression, and Survival Analysis*. 2001; Springer.
- [13] Koziol JA, Jia Z. The concordance index C and the Mann–Whitney parameter Pr (X > Y) with randomly censored data. *Biom J* 2009;51:467–74.
- [14] Xu D, Zhang S, Zhang S, et al. NOD2 maybe a biomarker for the survival of kidney cancer patients. *Oncotarget* 2017;8:101489–99.
- [15] Aguirre-Gamboa R, Gomez-Rueda H, Martínez-Ledesma E, et al. SurvExpress: an online biomarker validation tool and database for cancer gene expression data using survival analysis. *PLoS ONE* 2013;8:e74250.
- [16] Bovelstad HM, Borgon O. Assessment of evaluation criteria for survival prediction from genomic data. *Biom J* 2011;53:202–21.
- [17] Ostrom QT, Gittleman H, Liao P, et al. CBTRUS statistical report: primary brain and central nervous system tumors diagnosed in the United States in 2010–2014. *Neurooncology* 2014;16(suppl 4):1–63.
- [18] Stupp R, Mason WP, van den Bent MJ, et al. Radiotherapy plus concomitant and adjuvant temozolomide for glioblastoma. *N Engl J Med* 2005;352:987–96.
- [19] Ellis HP, Greenslade M, Powell B, et al. Current challenges in glioblastoma: intratumour heterogeneity, residual disease, and models to predict disease recurrence. *Front Oncol* 2015;5:251.
- [20] Rasmussen RD, Gajjar MK, Jensen KE, et al. Enhanced efficacy of combined HDAC and PARP targeting in glioblastoma. *Mol Oncol* 2016;10:751–63.
- [21] Network TC. Corrigendum: comprehensive genomic characterization defines human glioblastoma genes and core pathways. *Nature* 2013;494:506.
- [22] Cancer Genome Atlas Research Network. Comprehensive genomic characterization defines human glioblastoma genes and core pathways. *Nature* 2008;455:1061–8.
- [23] Li L, Wang B. Overexpression of microRNA-30b improves adenovirus-mediated p53 cancer gene therapy for laryngeal carcinoma. *Int J Mol Sci* 2014;15:19729–40.
- [24] Turner KM, Deshpande V, Beyter D, et al. Extrachromosomal oncogene amplification drives tumour evolution and genetic heterogeneity. *Nature* 2017;543:122–5.

- [25] Taylor-Weiner A, Zack T, O'Donnell E, et al. Genomic evolution and chemoresistance in germ-cell tumours. *Nature* 2016;540:114–8.
- [26] Gundem G, Van Loo P, Kremeyer B, et al. The evolutionary history of lethal metastatic prostate cancer. *Nature* 2015;520:353–7.
- [27] Verhaak RG, Hoadley KA, Purdom E, et al. Integrated genomic analysis identifies clinically relevant subtypes of glioblastoma characterized by abnormalities in PDGFRA, IDH1, EGFR, and NF1. *Cancer Cell* 2010;17:98–110.
- [28] Noushmehr H, Weisenberger DJ, Diefes K, et al. Identification of a CpG island methylator phenotype that defines a distinct subgroup of glioma. *Cancer Cell* 2010;17:510–22.
- [29] Phillips HS, Kharbanda S, Chen R, et al. Molecular subclasses of high-grade glioma predict prognosis, delineate a pattern of disease progression, and resemble stages in neurogenesis. *Cancer Cell* 2006;9:157–73.
- [30] Ferlay J, Shin HR, Bray F, et al. Estimates of worldwide burden of cancer in 2008: GLOBOCAN. *Int J Cancer* 2010;127:2893–917.
- [31] Linehan WM. Genetic basis of kidney cancer: role of genomics for the development of disease-based therapeutics. *Genome Res* 2012;22:2089–100.
- [32] Kong X, Kuilman T, Shahrabi A, et al. Cancer drug addiction is relayed by an ERK2-dependent phenotype switch. *Nature* 2017;550:270–4.
- [33] Nieto P, Ambrogio C, Esteban-Burgos L, et al. A Braf kinase-inactive mutant induces lung adenocarcinoma. *Nature* 2017;548:239–43.
- [34] Yao Z, Yaeger R, Rodrik-Outmezguine VS, et al. Tumours with class 3 BRAF mutants are sensitive to the inhibition of activated RAS. *Nature* 2017;548:234–8.
- [35] Kim J, Hu Z, Cai L, et al. CPS1 maintains pyrimidine pools and DNA synthesis in KRAS/LKB1-mutant lung cancer cells. *Nature* 2017;546:168–72.
- [36] Graziano P, de Marinis F, Gori B, et al. EGFR-driven behavior and intrapatient T790M mutation heterogeneity of non-small-cell carcinoma with squamous histology. *J Clin Oncol* 2015;33:e115–8.
- [37] Cai W, Lin D, Wu C, et al. Intratumoral heterogeneity of ALK-rearranged and ALK/EGFR coaltered lung adenocarcinoma. *J Clin Oncol* 2015;33:3701–9.
- [38] Kalemkerian GP, Narula N, Kennedy EB, et al. Molecular testing guideline for the selection of patients with lung cancer for treatment with targeted tyrosine kinase inhibitors: American Society of Clinical Oncology Endorsement of the College of American Pathologists/International Association for the Study of Lung Cancer/Association for Molecular Pathology Clinical Practice Guideline Update. *J Clin Oncol* 2018;36:911–9.
- [39] Leighl NB, Rekhtman N, Biermann WA, et al. Molecular testing for selection of patients with lung cancer for epidermal growth factor receptor and anaplastic lymphoma kinase tyrosine kinase inhibitors: American Society of Clinical Oncology endorsement of the College of American Pathologists/International Association for the study of lung cancer/association for molecular pathology guideline. *J Clin Oncol* 2014;32:3673–9.
- [40] Lee JK, Lee J, Kim S, et al. Clonal history and genetic predictors of transformation into small-cell carcinomas from lung adenocarcinomas. *J Clin Oncol* 2017;35:3065–74.
- [41] Mazières J, Zalcman G, Crinò L, et al. Crizotinib therapy for advanced lung adenocarcinoma and a ROS1 rearrangement: results from the EUROS1 cohort. *J Clin Oncol* 2015;33:992–9.
- [42] Blackhall FH, Peters S, Bubendorf L, et al. Prevalence and clinical outcomes for patients with ALK-positive resected stage I to III adenocarcinoma: results from the European Thoracic Oncology Platform Lungscape Project. *J Clin Oncol* 2014;32:2780–7.